*International Journal of Minerals, Metallurgy and Materials*
*Volume 25, Number 12, December 2018, Page 1363*
**https://doi.org/10.1007/s12613-018-1690-8**

# Characteristics and implications of stress state in a gold mine in Ludong area, China

*Peng Li*[1,2,3)], *Mei-feng Cai*[1,2,3)], *Qi-feng Guo*[1,2,3)], *and Sheng-jun Miao*[1,2,3)]

1) School of Civil and Resource Engineering, University of Science and Technology Beijing, Beijing 100083, China

2) Key Laboratory of High-Efficient Mining and Safety of Metal Mines (Ministry of Education of China), University of Science and Technology Beijing, Beijing 100083, China

3) Beijing Key Laboratory of Urban Underground Space Engineering, University of Science and Technology Beijing, Beijing 100083, China

(Received: 29 March 2018; revised: 13 June 2018; accepted: 7 August 2018)

**Abstract:** In this study, we obtained information from twenty-one measurement points on the stress magnitudes and orientations of a gold mine in the Ludong area. We used the overcoring technique with an improved hollow inclusion strain gauge and then analyzed the distribution characteristics of the *in situ* stress field. The results indicate that the stress field is characterized by $\sigma_H > \sigma_h > \sigma_v$ and $\sigma_H > \sigma_v > \sigma_h$ (where $\sigma_H$, $\sigma_h$, and $\sigma_v$ are the maximum horizontal, minimum horizontal, and vertical principal stresses, respectively). The regional stress field is dominated by horizontal principal stress. The $\sigma_H$, $\sigma_h$, and $\sigma_v$ values show a gradual increasing trend with depth. The $\sigma_H$ is predominantly oriented in the NWW–SEE or near-EW direction. We also confirmed the correspondence between the measured stress field and the regional geological structure. In addition, based on the measured stress data, we discuss the implications of the *in situ* stress with respect to fault activity in the mine area.

**Keywords:** *in situ* stress measurement; improved hollow inclusion strain gauge; stress field; geological structure; fault activity

## 1. Introduction

*In situ* stress, one of the most crucial and fundamental properties of the Earth's crust, is the natural stress that develops in crustal rock over the long time period of a geological process [1]. Changes in the stress state can lead to dynamic disasters in underground engineering works, and the stress state directly affects geological processes such as fault activity and earthquakes. In mining engineering, the entire process of excavation is controlled by the *in situ* stress. Hence, the *in situ* stress is the necessary mechanical boundary condition in the design and calculation of mining engineering projects. During the entire mining engineering service period, disasters such as the instability and failure of roadways, rock bursts, and roof collapses are closely related to changes in the stress state of the engineering rock mass. The stress state of the rock mass mainly depends on the *in situ* stress field, mining-induced stress field, and additional stress fields superimposed onto it. Of these, the magnitude and direction of the *in situ* stress field have a strong influence on the stress distribution in the surrounding rock. Therefore, knowledge of the characteristics of the *in situ* stress field in the rock mass at a given depth is essential for determining the mechanical properties of the engineering rock mass, analyzing the stability of the surrounding rock, and determining the regional fault stability. This knowledge facilitates the scientific design of and decision-making for excavation in mining engineering [2–3], and for safe and efficient mining, in particular.

The gold mine located in the northwestern Ludong area of Shandong Province, China—one of China's largest gold mines—extends from 120°07'30"–120°09'15" E longitude to 37°25'45"–37°27'00" N latitude. The main mining area is approximately 3.91 $km^2$ and the regional geological environment is very complex. The ore body of the gold mine is in the Jiaojia metallogenic belt, and multi-period tectonic movements and multi-stage mineralizations have led to complexities in the ore body morphology and occurrence

Corresponding author: Peng Li E-mail: lpxiaobudian@163.com

conditions that adversely affect mining. As mining activities increase in depth, the deep engineering geology conditions and ore deposit occurrences are increasingly complex and the surrounding rock pressure is significantly increased. Correspondingly, the frequency of dynamic disasters, such as rib spalling, collapse of the surrounding rock, roof collapse, and rock burst, obviously increase, which also seriously affects the ore recovery rate. As such, an accurate and complete understanding of the *in situ* stress field characteristics, the current condition of the geological structure and its migration, and the evolution rule in the mine area have great significance for solving key technical issues, such as the prediction and prevention of rock bursts in deep mining.

In this paper, we described the geological features of the northwest region of the mine area and present the results of our overcoring *in situ* stress measurements in the region. Next, we analyzed the distribution characteristics of the stress field and the relationship between the stress field and the geological structure. Finally, we discussed the fault activity that is occurring under the present stress state.

## 2. Geologic setting

The mine area comprises part of the Neocathaysian second uplift belt of the North China Platform and is located east of the Yishu fault zone, north of the Qixia anticlinorium, and at the southwestern tip of the Huangxian–Yexian arcuate fault zone. The *in situ* stress field of the mine area is generally controlled by the near-EW tectonic stress field of the North China Craton, and the geological structure of the mine area is mainly controlled by the regional EW trending tectonic system (such as the Qixia anticlinorium) and NE trending Neocathaysian fault structure (such as the Huangxian–Yexian arcuate fault zone). Geological investigation results have indicated that the Neocathaysian structure continues to be an active structural system. With respect to the stratigraphic regionalization, the mine area belongs to the Ludong Formation of the North China stratigraphic area, and the quaternary loose sediment in the Cenozoic is widely distributed. Most of the mine area is covered by Quaternary sediments, and magmatic rocks are widely exposed [4]. The scattered Archean Jiaodong Group metamorphic rocks, which occur as remnants in the magmatic rocks, are in intrusive contact or fault contact with Mesozoic magmatic rocks.

The main structures in the mine area are faults that are represented by the Jiaojia fault zone (Fig. 1). The Jiaojia fault zone runs through the entire mine area and is the most important ore-controlling structure of the gold deposit. It directly controls the formation of the ore body and its spatial distribution pattern. With a length of approximately 60 km, this fault zone strikes in the N35°–45°E direction, inclines in the NW direction, and is located in the southern extension of the Huangxian–Yexian arcuate fault zone. This fault zone is a large crushed zone composed of hornblende clastic rocks and granitic clastic rocks. The northern part of the fault zone developed in the contact zones of Guojialing

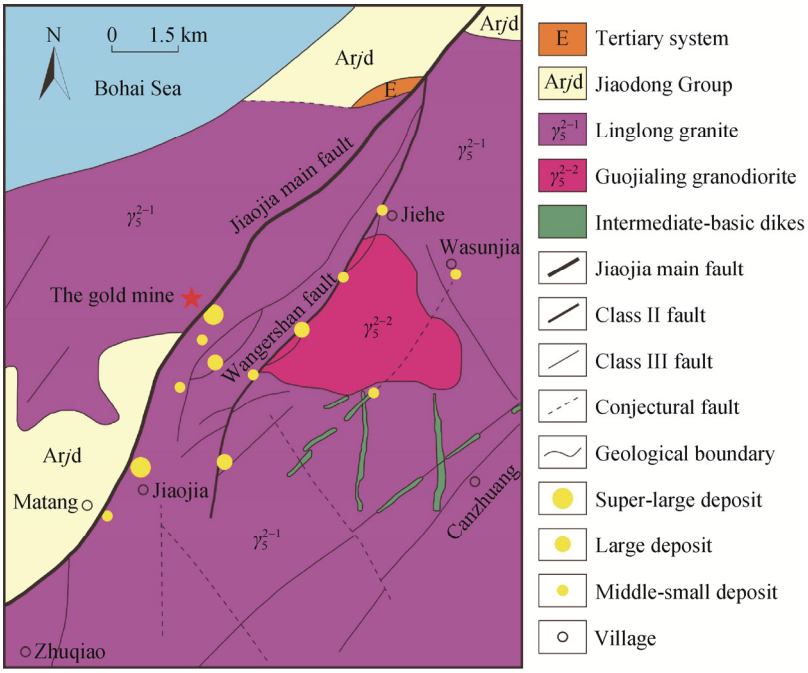


**Fig. 1. Simplified geological map of the mine area and its adjacent areas (modified after Ma [4]).**

granodiorite and Linglong granite and of Linglong granite and the Jiaodong Group, whereas the southern section mainly occurs in the Jiaodong Group. The fault zone is a multi-stage active composite fault zone with a wavy undulation in the main section and an "S" shaped distribution in the plane [5]. The secondary ore-controlling structures in the mine area are mainly in the North-east (NE), North-north-east (NNE), North-west (NW) directions and the secondary faults are parallel to the Jiaojia main fault. The famous Yishu fault zone located in the west of the mine area is the largest deep fault zone in Shandong Province and is currently still active, and shows an extremely noticeable fault control effect on the seismic activity in the region. Several earthquakes with magnitudes greater than 7.0 have occurred in the Yishu fault zone and adjacent areas. The northwestern Ludong area is the main seismic activity area in Eastern China, with earthquake magnitudes generally less than 5.0, and with the seismicity mainly affected by the Yishu fault zone. The most recent seismic event with a magnitude greater than 4.0 in the northwestern Ludong area was the Ms 4.6 Laizhou earthquake in 2013.

## 3. *In situ* stress measurement and results analysis

### 3.1. *In situ* stress measurement method and its results

To measure the *in situ* stress in the gold mine, we used a 3D stress relief method and an overcoring technique with an improved hollow-inclusion strain gauge. To increase the reliability and accuracy of the *in situ* stress measurement, we incorporated a full-temperature-compensation technique in the stress relief method, as proposed and designed by Cai *et al.* [6–7]. This technique included two main technical aspects: (1) continuous monitoring of the temperature change at the point of measurement during stress relief; and (2) the use of a temperature calibration test to measure the temperature strain rate (i.e., the strain value generated by a temperature change of 1°C) of the strain gauge at each measurement point. Therefore, the temperature calibration test was the most important part of the full-temperature-compensation technique. To apply this technique, we made significant improvements in the design and structure of the traditional hollow-inclusion strain gauge, as illustrated in Fig. 2. We also considered other improvements in the *in situ* measurements.

To ensure that all of the measurement points were located in the original rock stress area, their locations were far away from each other, the drilling depths exceeded three times the roadway span, and the measurement points were more than 50 m from the adjacent roadway or other excavation works. Using the methods described by Cai *et al.* [7], we obtained seventeen sets of data from 1991 to 1993 and four later sets of data, which are presented in Table 1. As we can see in the table, two of the three principal stresses are nearly horizontal, with the absolute values of the dip angles generally less than 10°, whereas the other principal stress is nearly vertical, with a minimum dip angle of 70.04°. The two principal stresses in the near-horizontal direction are called the

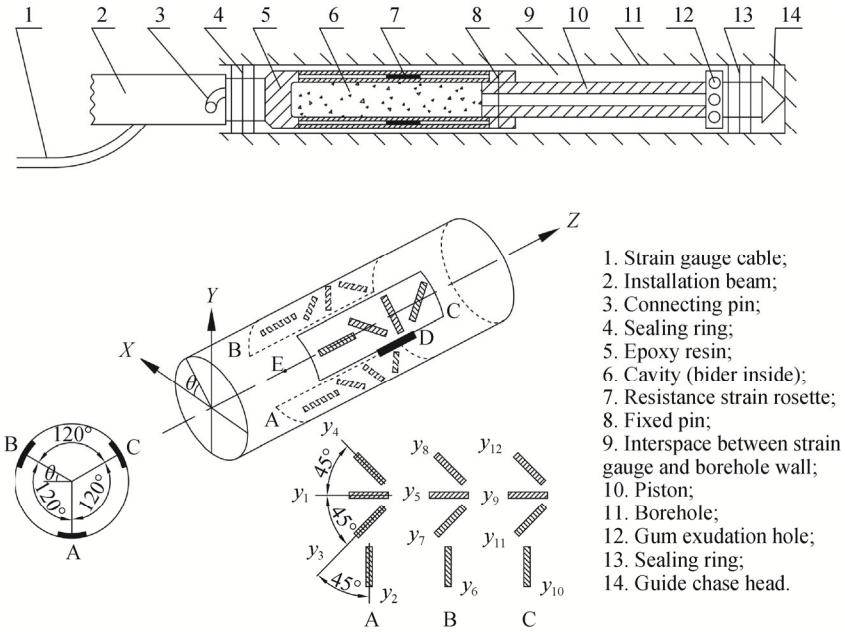


**Fig. 2. Sketch of the improved hollow inclusion strain gauge used to ensure full temperature compensation.**

**Table 1. Results of *in situ* stress measurements in the gold mine**

| No. | Depth / m | Maximum principal stress, $\sigma_1$ | | | Intermediate principal stress, $\sigma_2$ | | | Minimum principal stress, $\sigma_3$ | | |
|---|---|---|---|---|---|---|---|---|---|---|
| | | Value / MPa | Direction / (°) | Dip / (°) | Value / MPa | Direction / (°) | Dip / (°) | Value / MPa | Direction / (°) | Dip / (°) |
| 1 | 205 | 11.45 | 307.1 | −17.6 | 5.69 | 286.3 | 71.3 | 4.03 | 35.1 | 6.2 |
| 2 | 205 | 11.54 | 270.0 | 4.3 | 6.77 | 181.5 | −19.0 | 5.72 | 347.8 | −70.04 |
| 3 | 205 | 11.27 | 218.9 | 10.2 | 5.68 | 220.2 | −79.8 | 3.98 | 129 | −0.2 |
| 4 | 235 | 14.62 | 237.6 | 9.2 | 10.17 | 329.9 | 13.9 | 5.63 | 295.1 | −73.2 |
| 5 | 235 | 13.69 | 128.7 | −7.8 | 6.83 | 131.3 | 82.2 | 5.06 | 38.8 | 0.3 |
| 6 | 235 | 12.99 | 301.9 | −0.6 | 6.14 | 208.2 | −81.3 | 5.00 | 212.0 | 8.7 |
| 7 | 235 | 13.60 | 311.0 | −1.4 | 8.93 | 220.7 | −10.4 | 6.85 | 228.8 | 79.5 |
| 8 | 235 | 12.58 | 280.0 | −13.2 | 7.85 | 187.3 | −11.1 | 6.92 | 238.5 | 72.6 |
| 9 | 235 | 12.80 | 127.1 | −7.2 | 7.41 | 35.9 | −9.7 | 5.89 | 72.4 | 78.0 |
| 10 | 310 | 17.63 | 119.0 | −2.1 | 11.65 | 209.2 | −4.7 | 10.73 | 185.6 | 84.8 |
| 11 | 310 | 18.50 | 285.5 | −17.7 | 8.89 | 80.8 | −70.6 | 7.05 | 13.0 | 7.6 |
| 12 | 310 | 18.39 | 123.1 | −1.6 | 11.65 | 213.2 | −3.3 | 10.73 | 187.7 | 86.4 |
| 13 | 310 | 20.73 | 109.9 | −0.4 | 9.00 | 201.9 | −79.1 | 7.01 | 199.8 | 10.9 |
| 14 | 310 | 16.32 | 82.9 | 3.2 | 9.19 | 13 | −80.7 | 7.99 | 172.4 | −8.7 |
| 15 | 410 | 29.62 | 308.9 | −5.3 | 13.77 | 193.2 | −78.0 | 11.98 | 219.9 | 10.7 |
| 16 | 410 | 31.49 | 148.4 | −6.9 | 14.13 | 267.7 | −76.0 | 11.08 | 236.9 | 12.0 |
| 17 | 410 | 31.55 | 327.2 | 11.77 | 13.89 | 219 | −79.1 | 11.77 | 237.8 | 10.3 |
| 18 | 410 | 25.98 | 90.7 | −4.5 | 11.54 | 106.7 | 85.3 | 5.78 | 0.8 | 1.3 |
| 19 | 610 | 30.21 | 300 | −22 | 17.12 | 357 | −72 | 13.09 | 28 | 15 |
| 20 | 660 | 33.35 | 280 | −9 | 21.46 | 322 | −78 | 20.08 | 11 | 8 |
| 21 | 660 | 31.68 | 276 | −10 | 19.04 | 252 | −80 | 16.55 | 9 | 6 |

maximum horizontal principal stress ($\sigma_H$) and minimum horizontal principal stress ($\sigma_h$); and the principal stress close to the vertical direction is called the vertical principal stress ($\sigma_v$). The depths of the twenty-one measurement points ranged from 205 to 660 m. These stress data can not only help to solve mining engineering problems but are also of great value in the study of the regional tectonic stress field in the mine area.

### 3.2. Characteristics of *in situ* stress field

3.2.1. Magnitude of the principal stresses

Fig. 3 shows the *in situ* stress magnitudes as a function of depth ($H$), which we derived from the 21 tests in the gold mine. Due to a variety of influence factors, such as inconsistencies in the testing procedures and effects of the local geology, including different lithologies, there are some discrepancies in the stress data. From Fig. 3, we can see that despite the scattered nature of the measurement results, the principal stresses ($\sigma_H$, $\sigma_h$, and $\sigma_v$) show a gradual increasing trend with depth in the shallow crust. A linear expression fits these data well, as shown in Fig. 3. The values of the horizontal principal stress in all of the tests are definitely higher than those of the vertical principal stress, which suggests that the stress field is dominated by horizontal principal stress. Moreover, the vertical principal stress is approximately equal to the overburden weight. We found that the fitting expressions for the principal stresses given in Fig. 3 comprise a model of the *in situ* stress field in the mine area, and can provide stress boundary conditions for the underground excavation design, stability evaluation, and support systems optimization.

According to Anderson's theory of faulting [8], for a normal fault, $\sigma_v > \sigma_H > \sigma_h$; for a thrust fault, $\sigma_H > \sigma_h > \sigma_v$; and for a strike-slip fault, $\sigma_H > \sigma_v > \sigma_h$. As we can see in Table 1, 7 of the 21 measurement points follow a thrust faulting stress regime and the other 14 a strike-slip faulting stress regime. Furthermore, as shown in Fig. 3, there is a piecewise distribution of the principal stresses that approximately estimates the stress regime of the mine area in two zones. At shallow (< 223 m) and medium (> 223 m) depths, the stress regimes can be characterized as $\sigma_H > \sigma_h > \sigma_v$ and $\sigma_H > \sigma_v > \sigma_h$, respectively. The stress regime changes with depth because as depth increases, the dominant role of the horizontal tectonic stress field weakens, and the role of the vertical stress is enhanced.

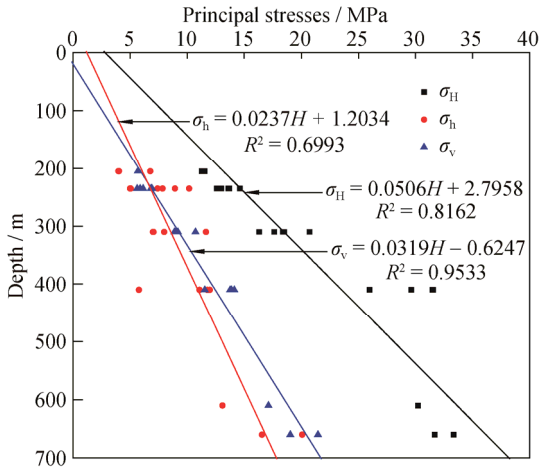


**Fig. 3. Regression lines of the principal stresses with depth.**

In addition to the principal stresses, Fig. 4 shows a plot of the magnitudes of the *in situ* stress ratios, as determined from the measured stress data as a function of depth. Because the $\sigma_H$ magnitudes depend to some extent on the $\sigma_h$ values, the profiles in Figs. 4(a) and 4(b) are almost identical. The ratio of $\sigma_H$ to $\sigma_v$ ($K_{Hv}$) is between 1.55 and 2.60, with an average value of 2.00. Overall, we can see that the dispersion and values of $K_{Hv}$ decrease non-linearly with depth (Fig. 4(a)). The ratio of the average horizontal principal stress to the vertical principal stress, i.e., $K_{av} = (\sigma_H + \sigma_h) / 2\sigma_v$, is in the range of 1.24 to 2.20, with an average value of 1.47, and shows considerable scattering. The $K_{av}$ value is greater at shallow depths and gradually decreases with depth (Fig. 4(b)), which indicates that the difference between the three principal stresses narrows with depth and that the dominant role of the horizontal tectonic stress field weakens as the role of the vertical principal stress is enhanced. The variation law of $K_{av}$ with respect to depth (Fig. 4(b)) in the mine area is similar to that of the global variation law interpreted by Brown and Hoek [9]. However, there is a significant difference between the magnitudes of the values. This difference may be attributed to one of two reasons. It may be because the stress measurement data obtained by Brown and Hoek [9] cover a number of different test sites in many counties and have various geological features, tectonic movements, and rock types. These factors will result in a large scattering of the stress measurement data compared to those obtained from a specific site. On the other hand, extremely large differences in the measurement depth between

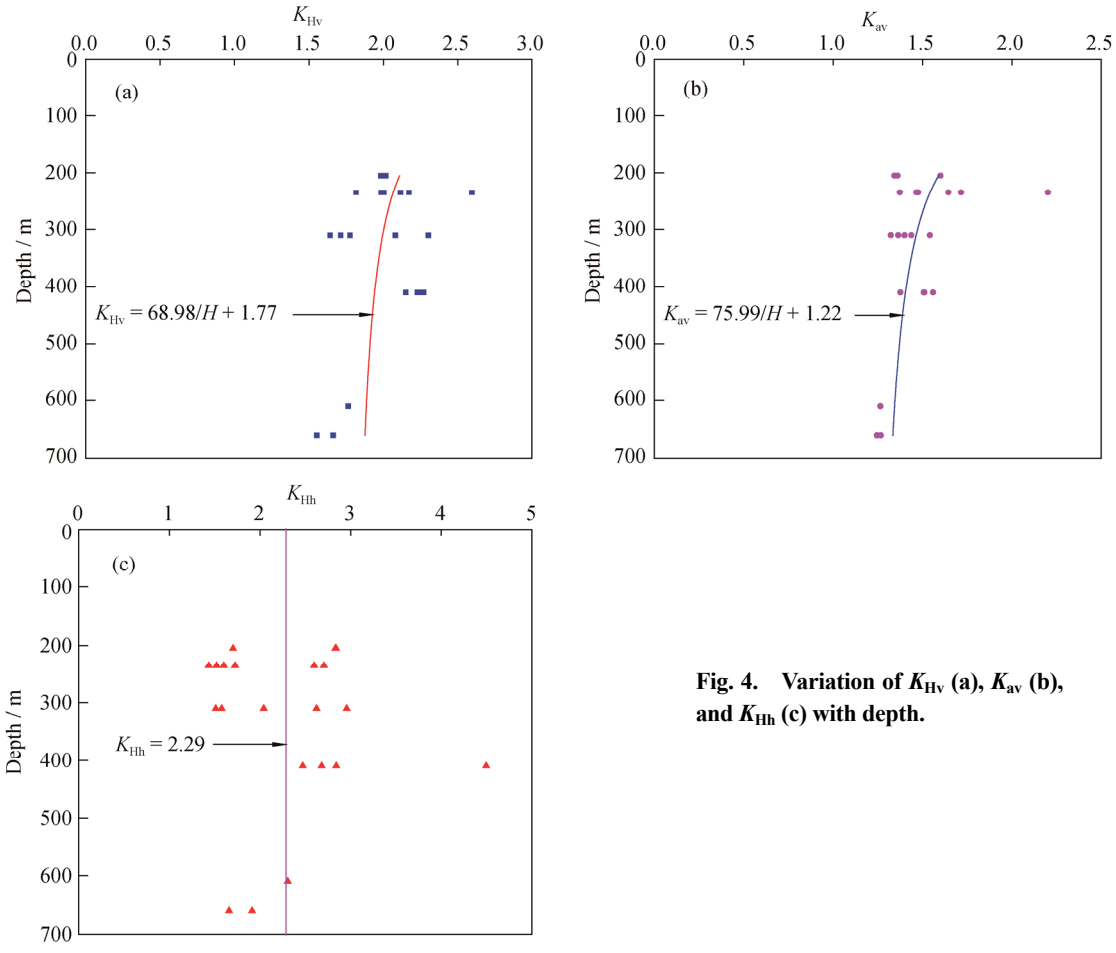


**Fig. 4. Variation of $K_{Hv}$ (a), $K_{av}$ (b), and $K_{Hh}$ (c) with depth.**

projects may significantly affect the fitting results of the stress data. We found the features of the tectonic stress fields formed in various regions to be very different. The ratio of $\sigma_H$ to $\sigma_h$ ($K_{Hh}$) is in the range of 1.44 to 4.49 and varies remarkably with depth. The difference between the maximum and minimum horizontal principal stresses is significant, with an average value of 2.29 (Fig. 4(c)). According to the Mohr-Coulomb strength theory, the difference between $\sigma_H$ and $\sigma_h$ is the shear stress, which is the major causal factor in the deformation and failure of underground roadways and stopes and must be more carefully monitored. In addition, the large shear stress in the Earth's crust is one of the key mechanical factors leading to the relative development and dense distribution of faults, joints, and other structures in the mine area.

3.2.2. *In situ* stress field orientation

Fig. 5 shows the orientation of $\sigma_H$ and $\sigma_h$ in the mine area. As shown in Fig. 5(a), among the 21 measurement points, 18 $\sigma_H$ points lie along the NW–SE direction, 16 of which are concentrated along the NWW–SEE or near-EW direction, and the remaining 3 $\sigma_H$ points are in the NE–SW direction. We can conclude that the $\sigma_H$ in the mine area is predominantly oriented in the NWW–SEE or near-EW direction. The maximum horizontal principal stresses generally strike coincidentally with the maximum stress direction of the regional tectonic stress field, as interpreted by the neotectonic activity. Under the action of the NWW–SEE or near-EW trending regional tectonic stress field, the motions of the NE–NEE trending faults in the mine area are mainly subjected to dextral strike-slip, which coincides with the current movement, which is dominated by the dextral strike-slip of the Jiaojia fault zone. On the other hand, among the 21 measurement points, 18 $\sigma_h$ points lie in the NE–SW direction (Fig. 5(b)). Thus, we can conclude that the regional *in situ* stress field in the mine area is influenced by NWW–SEE or near-EW trending tectonic stress.

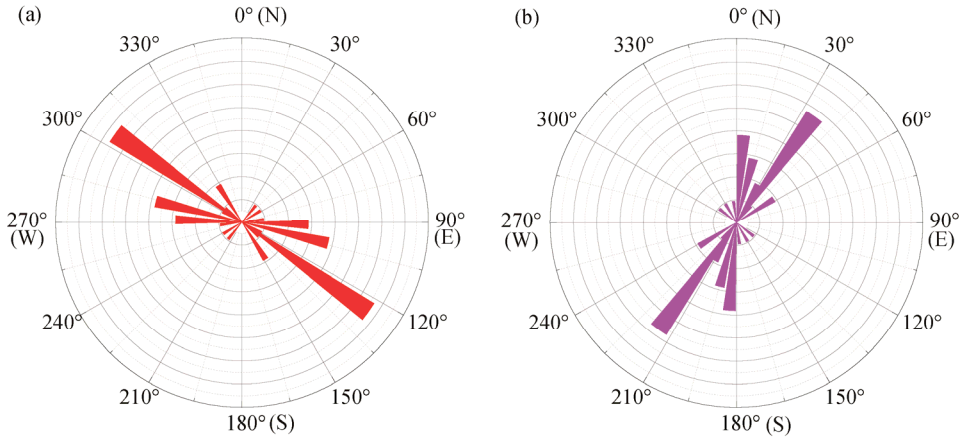


**Fig. 5. Orientations of $\sigma_H$ (a) and $\sigma_h$ (b) in the mine area.**

Fig. 6 shows the distribution characteristics of the modern tectonic stress field in the North China block, based on the movements of the tectonic plates, focal mechanism solutions, *in situ* stress measurement results, and other geological indicators [10]. As we can see from Fig. 6, the inferred overall direction of the maximum horizontal principal stress in the mine area is in the NWW–SEE or near-EW direction, which is approximately consistent with the measured results in the mine area (Fig. 5(a)). This result indicates that the stress field inferred from overcoring measurements can accurately reflect the current stress state in the mine area. Furthermore, it provides evidence that the stress measurement results obtained from the mine area support the hypothesis of the horizontal compressive stress origin in the northwestern Ludong area and that the stress field in the northwestern Ludong area is dominated by the Philippine and Pacific plates rather than the Indian plate. We note that due to the existence of local faults, there are also some local stress fields that exhibit a certain deviation from the dominant orientation of the overall stress field in the region. Therefore, we must comprehensively evaluate the tectonic stress field in the mine area in combination with *in situ* stress measurements.

## 4. Relationship between the *in situ* stress field and geological structure

The *in situ* stress field develops in a dynamic evolutionary process, and the principal stress orientation is significantly affected by geological structures that range in size from microcracks to major faults. The influence range of the geological structures on the stress field is directly proportional to their sizes. In turn, most of the geological structures

in the strata are the result of various tectonic movements driven by crustal stress. The geological structures that form under different stress conditions tend to differ, and, to a certain degree, a diversity of geological formations can reflect different tectonic stress states at the time of their formation. When the current stress field overlaps with the previous stress field and develops further or is coupled with a historical tectonic stress field, the new and the old structural systems may interact and form a relationship [11]. Therefore, we can gain insight into the regional tectonic stress by investigating the relationship between the *in situ* stress field and the geological structures within a specific area.

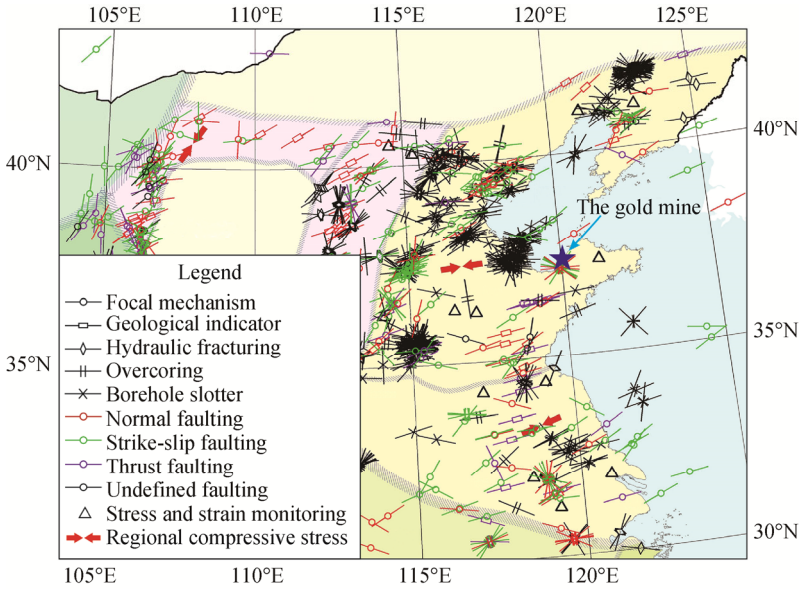


**Fig. 6. Modern tectonic stress field map of the North China block (modified after Han *et al.* [10]).**

As mentioned above, the mine area comprises part of the Neocathaysian second uplift belt of the North China Platform, an area that has experienced in succession a sedimentary stage, Jiaodong movement, Penglai movement, Yanshan movement, and Himalayan tectonic movement throughout geological history. Based on the formation time, the structure of the mine area can be divided into an EW-trending tectonic structure and Neocathaysian structural system. The development mode of the *in situ* stress field and the current stress state in the mine area are likely to be the result of these two tectonic systems working together in this area.

The EW-trending Qixia anticlinorium in the Archean and Proterozoic strata is the main geological framework of the mine area, and the direction of the principal compressive stress corresponding to the tectonic period is South-north (SN). The Neocathaysian structural system can be divided into early and late stages [11]. The Neocathaysian structural system is an extremely important and magnificent tectonic system with respect to the metallogenic control and structural layout that have affected mountain landforms since the Yanshan movement, and is found in almost all regions of the eastern Chinese mainland. The Neocathaysian structural system is currently a very active tectonic system, and its activities are tending to gradually increase. The Neocathaysian structural system transforms pre-generated structural planes, influences and controls the development of geomorphic systems, and has a wide distribution of seismicity. The early Neocathaysian structural system evolved from the NE-trending tectonic structure of the Jurassic era and was formed by lateral pressure in the NW–SE-direction. The early Neocathaysian structural system is a direct control structure of the ore body in the mine area. In particular, its interaction or joints with other tectonic systems show more obvious control of the deposits. Fig. 7 shows the tectonic evolution of faults in the mine area, and we can see that the ore-controlling faults in the NNE-direction are extended in a near parallel fashion. These are a set of NWW–SEE extensional fault tectonic systems on the plane that combine a gentle sloping fault and secondary tensile fissure in the section. The joint development of the primary and secondary faults is the general evolutionary feature of the fault structure in this area [5]. The late Neocathaysian structural system formed from NNE-trending faults after the Cretaceous age and affects the metallogenic regularity of the region. The late Neocathaysian structural system often overlapped with the early Neocathaysian structural system, which were both formed by principal-stress axis rotations in different periods under the same stress field. Therefore, we can infer

that the direction of the maximum principal stress of the tectonic stress field in the mine area changed from the earlier SN-trend to the NWW-trend and continues to deflect in an EW-deflection.

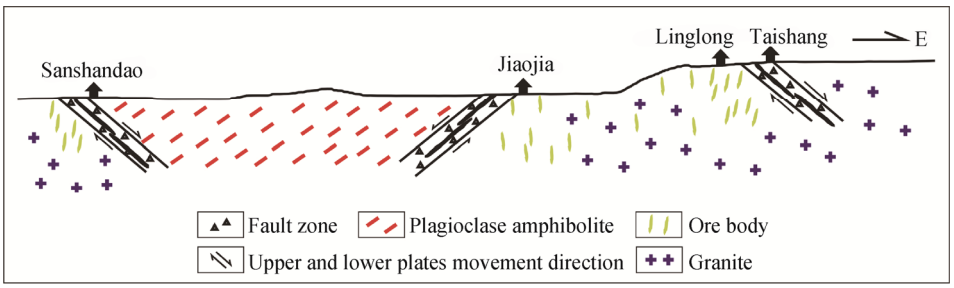


**Fig. 7. Sketch map of the tectonic evolution of the faults in the mine area (modified after Shen [5]).**

Furthermore, geological studies have shown that the stress field in a mine area mainly inherits the tectonic stress field of the Neocathaysian structural system and is controlled by the tectonic stress field, for which the principal compressive stress direction is NWW–SEE [6]. Hence, we can see that the dominant orientation of the maximum principal compressive stress in the mine area is consistent with the direction of the tectonic stress field of the Neocathaysian structural system. This finding is in agreement with the hypothesis that the stress state in an area is mainly controlled by the latest tectogenesis, and especially the active tectogenesis in this area. On the other hand, this result strongly supports the mechanisms of the origin of the Neocathaysian structural system and shows that the stress measurement results are accurate and reliable.

In conclusion, we can deduce that the formation and development of the faults in the mine area are due to the tectonic activities of the Neocathaysian structural system and that the distribution of the stress field in the mine area is a reflection of the historical and current characteristics of the tectonic movement in this area. Thus, we confirm the consistency between the measured *in situ* stress field and the regional geological structure.

## 5. Implications of *in situ* stress for fault activity

Fault activity is an important factor for evaluating crustal stability. The Earth's crust is in a critical equilibrium state as faults slip or earthquakes occur [12]. Previous studies have shown that the activity of a fault is mainly controlled by its stress state [13–14]. Hence, here, we discuss the implications of *in situ* stress for fault activity in the mine area based on *in situ* stress measurements. To analyze the current activity characteristics and potential development trend of the fault in the mine area, we selected the ratio of half of the maximum horizontal differential stress to the average horizontal principal stress ($\mu_d$) and the stress factor ($K$) as parameters in our stress characteristics analysis, based on the measured stress data. We calculated $\mu_d$ and $K$ as follows:

$$\mu_d = (\sigma_1 - \sigma_3)/(\sigma_1 + \sigma_3) \quad (1)$$

$$K = (\sigma_1 - \sigma_2)/(\sigma_1 - \sigma_3) \quad (2)$$

where $\mu_d$ is the ratio of the average shear stress $(\sigma_1 - \sigma_3)/2$ to the average principal stress $(\sigma_1 + \sigma_3)/2$, and $K$ is the stress factor of the relative relationship between the three principal stresses. For a thrust fault, $\sigma_1$ and $\sigma_3$ are equal to $\sigma_H$ and $\sigma_v$, respectively, and for a strike-slip fault, $\sigma_1$ and $\sigma_3$ are equal to $\sigma_H$ and $\sigma_h$, respectively.

$\mu_d$ is a parameter related to the crustal failure state and can describe the state of the crustal shear stress as well as the weight stress build-up in the upper crust [15–17]. A larger $\mu_d$ value means a higher shear stress accumulation, which facilitates fault sliding, and vice versa. The $\mu_d$ value in the crust should generally not exceed 0.50–0.70; otherwise, shear failure may occur [16–17]. On the other hand, $K$ can reflect whether the correlation of $\sigma_1$, $\sigma_2$, and $\sigma_3$ is favorable for fault slip. For the best-fit stress model, a fault may be caused to slip if the value of $K$ is estimated to be approximately 0.5, i.e., and the magnitude of $\sigma_2$ is nearly the average of the magnitudes of $\sigma_1$ and $\sigma_3$ [18].

In this study, the average $\mu_d$ and $K$ values we calculated from the measured stress data were 0.40, and 0.81, respectively. The results shown in Fig. 8(a) reveal that the values of $\mu_d$ and $K$ are approximately linear, i.e., the constant values of $\mu_d = 0.40$ and $K = 0.81$ can be used to express the trends of $\mu_d$ and $K$ with respect to depth, respectively. Fig. 8(b) shows the fitting equation for $(\sigma_1 - \sigma_3)$ and $(\sigma_1 + \sigma_3)$, namely, $(\sigma_1 - \sigma_3) = 0.39(\sigma_1 + \sigma_3)$, and the slope of the fitting line is basically the same as the average value of $\mu_d$. We can see that the values of $\mu_d$ in most of the measurement depth ranges did not exceed the lower limit of the critical value of $\mu_d = 0.50$, which indicates that the faults in the mine area are less likely to be reactivated today. The fitting equation for $(\sigma_1 - \sigma_2)$ and $(\sigma_1 - \sigma_3)$ is given in Fig. 8(c), i.e., $(\sigma_1 - \sigma_2) =$

$0.82(\sigma_1 - \sigma_3)$, and the slope of the fitted line is almost equal to the average value of $K$. The $K$ values at almost all measured depths are far greater than 0.50, which implies that the relationship between the three principal stresses is not in the best-fit stress model for generating fault slipping, i.e., the stress state is not conducive to fault activity in the mine area. In summary, we can conclude that the results obtained by the above two methods are basically consistent, that is, the faults in the mine area are in a relatively stable state, given the current tectonic stress state. We note that we performed a preliminary quantitative analysis of the fault activity from the perspective of the *in situ* stress, and the conclusions we obtained inevitably have certain limitations. To fully understand the fault activities in the mine area, further research will be necessary with reference to related fields, including seismogeology, geophysics, and plate tectonics.

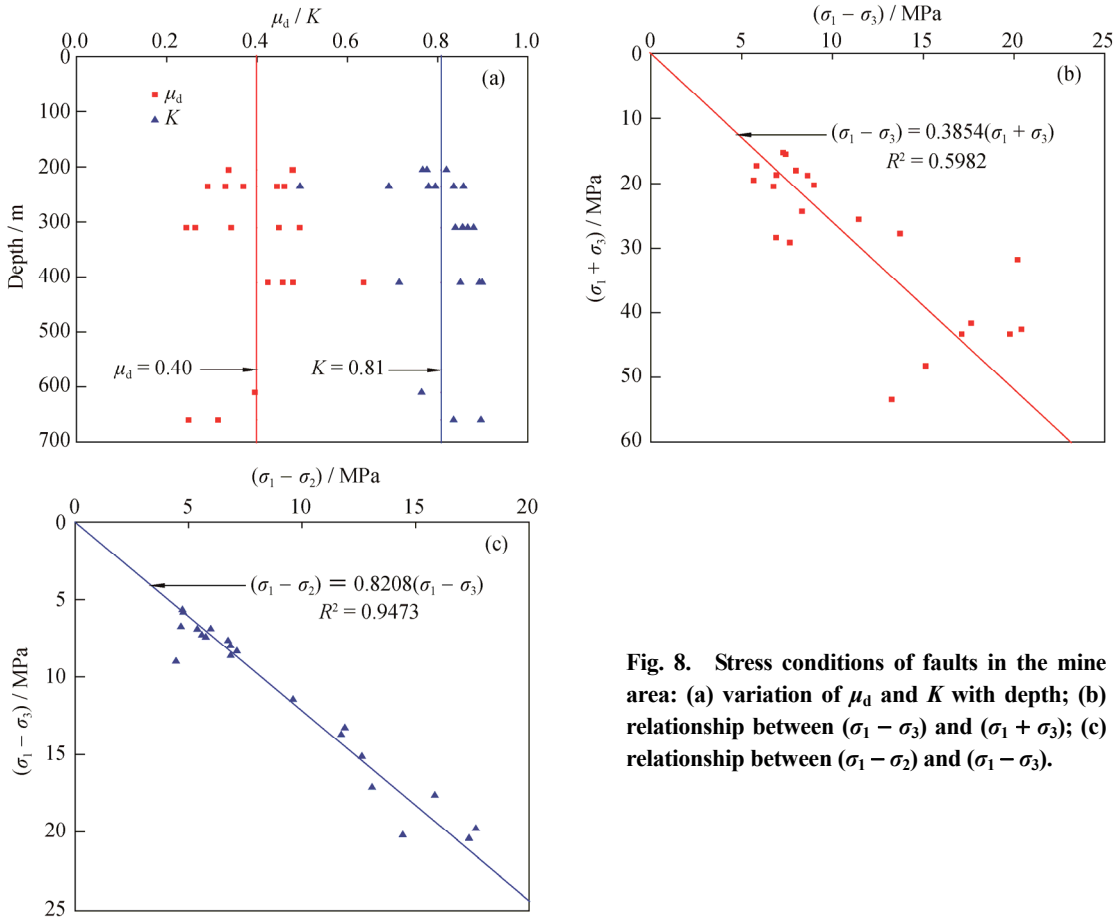


**Fig. 8. Stress conditions of faults in the mine area: (a) variation of $\mu_d$ and $K$ with depth; (b) relationship between $(\sigma_1 - \sigma_3)$ and $(\sigma_1 + \sigma_3)$; (c) relationship between $(\sigma_1 - \sigma_2)$ and $(\sigma_1 - \sigma_3)$.**

## 6. Conclusions

(1) The principal stresses ($\sigma_H$, $\sigma_h$, and $\sigma_v$) show a gradual increasing trend with depth. The regional stress field is dominated by the horizontal tectonic stress. The stress regime can be characterized as $\sigma_H > \sigma_h > \sigma_v$ and $\sigma_H > \sigma_v > \sigma_h$. Overall, the $K_{av}$ and $K_{Hv}$ values are greater at shallow depths and decrease non-linearly with depth. $K_{Hh}$ ranges from 1.44 to 4.49 and only varies slightly with depth.

(2) The measured maximum principal compressive stress in the mine area is mainly oriented in the NWW–SEE or near-EW direction, which basically coincides with the maximum stress direction of the regional tectonic stress field, as interpreted by the neotectonic activity, and is generally consistent with the orientation of the modern tectonic stress field in the North China block. The direction of the maximum principal stress of the tectonic stress field in the mine area has changed from the earlier SN-direction to the NWW-direction and continues to deflect in an EW-deflection. The dominant orientation in the mine area is also consistent with the direction of the tectonic stress field in the Neocathaysian structural system. The measured results strongly support the mechanisms of the origin of the Neocathaysian structural system and indicate that the stress measurement results are accurate and reliable.

(3) The values of $\mu_d$ in most of the measurement depth ranges did not exceed the lower limit of the critical value of $\mu_d = 0.50$, which indicates that the faults in the mine area are

currently unlikely to be reactivated. The $K$ values at almost all measured depths are far greater than 0.50, which implies that the relationship between the three principal stresses does not follow the best-fit stress model to cause fault slipping. We can conclude that the faults in the mine area are in a relatively stable state, given the present tectonic stress state.

## Acknowledgements

This work was financially supported by the State Key Research Development Program of China (Nos. 2016YFC0600801, 2017YFC0804103, and 2016YFC0600703), and the National Key Basic Research Program of China (973 Program) (No. 2015CB060200).

## References

[1] R. Liu, J.Z. Liu, W.L. Zhu, F. Hao, Y.H. Xie, Z.F. Wang, and L.F. Wang, *In situ* stress analysis in the Yinggehai Basin, northwestern South China Sea: Implication for the pore pressure-stress coupling process, *Mar. Pet. Geol.*, 77(2016), p. 341.

[2] P. Li, Q.F. Guo, S.J. Miao, and M.F. Cai, Comparisons of *in-situ* stress fields and stability of faults in shallow and deep engineering areas, *J. Harbin Inst. Technol.*, 49(2017), No. 9, p. 10.

[3] K. Li, Y.Y. Wang, and X.C. Huang, DDM regression analysis of the *in-situ* stress field in a non-linear fault zone, *Int. J. Miner. Metall. Mater.*, 19(2012), No. 7, p. 567.

[4] X.D. Ma, *Structure-Alteration-Mineralization Network of Xincheng Gold Deposit, Jiaodong Peninsula* [Dissertation], China University of Geosciences (Beijing), Beijing, 2011, p. 9.

[5] Y.K. Shen, *Study on Tectono-Alteration Net of Gold in Northwest Jiaodong* [Dissertation], China University of Geosciences (Beijing), Beijing, 2006, p. 15.

[6] M.F. Cai, L. Qiao, C.H. Li, J. Yu, B. Yu, and G. Chen, Application of an improved hollow inclusion technique for *in situ* stress measurement in Xincheng Gold Mine, China, *Int. J. Rock Mech. Min. Sci. Geomech. Abstr.*, 7(1995), No. 32, p. 735.

[7] M.F. Cai, L. Qiao, and C.H. Li, Measuring results and regularity of *in situ* stress in Xincheng gold mine, *Nonferrous Met.*, 52(2000), No. 3, p. 1.

[8] E.M. Anderson, *The Dynamics of Faulting and Dyke Formation with Applications to Britain*, Hafner Pub. Co., New York, 1951, p. 1.

[9] E.T. Brown and E. Hoek, Trends in relationships between measured *in situ* stresses and depth, *Int. J. Rock Mech. Min. Sci. Geomech. Abstr.*, 15(1978), No. 4, p. 211.

[10] J. Han, H.W. Zhang, B. Liang, H. Rong, T.W. Lan, Y.Z. Liu, and T. Ren, Influence of large syncline on *in situ* stress field: A case study of the Kaiping coalfield, China, *Rock Mech. Rock Eng.*, 49(2016), No. 11, p. 4423.

[11] S.J. Miao, Y. Li, W.H. Tan, and F.H. Ren, Relation between the *in-situ* stress field and geological tectonics of a gold mine area in Jiaodong Peninsula, China, *Int. J. Rock Mech. Min. Sci.*, 51(2012), No. 4, p. 76.

[12] M.L. Wu, C.Y. Zhang, and T.Y. Fan, Stress state of the Baoxing segment of the southwestern Longmenshan Fault Zone before and after the Ms 7.0 Lushan earthquake, *J. Asian Earth Sci.*, 121(2016), p. 9.

[13] J. Townend and M.D. Zoback, How faulting keeps the crust strong, *Geology*, 28(2000), No. 5, p. 399.

[14] J.D.O. Williams, M.W. Fellgett, and M.F. Quinn, Carbon dioxide storage in the Captain Sandstone aquifer: determination of *in situ* stresses and fault-stability analysis, *Pet. Geosci.*, (22)2016, No. 3, p. 211.

[15] D.B. Jamison and N.G.W. Cook, Note on measured values for the state of stress in the Earth's crust, *J. Geophys. Res. Solid Earth*, 85(1980), No. B4, p. 1833.

[16] Y.H. Wang, X.F. Cui, X.P. Hu, and F.R. Xie, Study on the stress state in upper crust of China mainland based on *in-situ* stress measurements, *Chin. J. Geophys.*, 55(2012), No. 9, p. 3016.

[17] C.H. Wang, C.K. Song, Q.L. Guo, Y.S. Zhang, and J.M. Ding, Stress build-up in the shallow crust before the Lushan Earthquake based on the *in situ* stress measurements, *Chin. J. Geophys.*, 57(2014), No. 3, p. 369.

[18] C.D. Chang, J.B. Lee, and T.S. Kang, Interaction between regional stress state and faults: Complementary analysis of borehole *in situ* stress and earthquake focal mechanism in southeastern Korea, *Tectonophysics*, 485(2010), No. 1-4, p. 164.